ResearchGate

See discussions, stats, and author profiles for this publication at: https://www.researchgate.net/publication/259313616

Anisotropic Mo 2 −Phthalocyanine Sheet: A New Member of the Organometallic Family

ARTICLE *in* THE JOURNAL OF PHYSICAL CHEMISTRY A · DECEMBER 2013

Impact Factor: 2.69 · DOI: 10.1021/jp4109255 · Source: PubMed

CITATIONS
2

READS
37

4 AUTHORS, INCLUDING:

Guizhi Zhu
Peking University
5 PUBLICATIONS **19** CITATIONS
SEE PROFILE

Qiang Sun
80 PUBLICATIONS **2,382** CITATIONS
SEE PROFILE

Available from: Guizhi Zhu
Retrieved on: 26 January 2016

THE JOURNAL OF PHYSICAL CHEMISTRY A

Article

pubs.acs.org/JPCA

Anisotropic Mo_2–Phthalocyanine Sheet: A New Member of the Organometallic Family

Guizhi Zhu,[†] Min Kan,[†] Qiang Sun,*[,†,‡,§] and Puru Jena[§]

[†]Department of Materials Science and Engineering, Peking University, Beijing 100871, China

[‡]Center for Applied Physics and Technology, Peking University, Beijing 100871, China

[§]Department of Physics, Virginia Commonwealth University, Richmond, Virginia 23284, United States

ABSTRACT: Metal–organic porous sheets, due to their unique atomic configurations and properties, represent a class of materials beyond graphene and BN monolayers. The Mo_2–phthalocyanine-based sheet (Mo_2Pc) is a new member of this porous organometallic family. Using density functional theory with hybrid functional for exchange–correlation potential, we show that this dimer-based material, unlike conventional organic monolayers that contain isolated metal atoms, possesses unique mechanical, magnetic, electronic, and optical properties due to inherent anisotropy in the structure. Furthermore, it is a semiconductor with a direct band gap of 0.93 eV and is antiferromagnetic with each Mo site carrying a magnetic moment of 0.88 μ_B. The strong anisotropy in elasticity and infrared light absorption is likely to open new doors for potential applications.

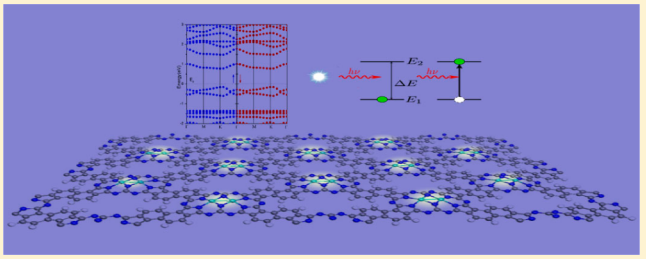

I. INTRODUCTION

Among two-dimensional (2D) monolayer materials, organometallic porous sheets have recently attracted considerable attention due to their flexibility in synthesis, well-defined geometry, and promising applications in hydrogen storage, electronic circuits, nonlinear optics, cancer therapy, quantum Hall effect, and spintronics.[1−6] Among these, phthalocyanines (Pcs) are ideal templates. The pores in these organic materials allow the flexibility of embedding metal atoms or complexes. When exposed to transition metal atoms or metal salts, the metallo-Pcs form planar systems with D_{4h} symmetry and the metal atom connected to four isoindole rings. The successful synthesis of the 2D Fe–phthalocyanine-based (poly-FePc) sheet paved the way for exploring 2D organometallic materials where the metal species are replaced with other elements showing flexibility and diversity.[7] For example, when boron or uranium ions are reacted with a phthalonitrile, structures consisting of three isoindole rings (SubPcs) or five isoindole rings (SuperPcs) are formed. Until recently, all the metallo-Pcs, SubPcs, and SuperPcs reported contain isoindole rings connected by aza nitrogen atoms. Recently, Matsushita et al.[8] synthesized an expanded Pc congener containing a Mo_2 dimer and four isoindole moieties and characterized it through a variety of methods such as electrochemistry, mass spectrometry, IR, electron paramagnetic resonance, NMR, and X-ray diffraction. These expanded metallo-Pcs form the basis of another class of 2D materials that go beyond graphene, BN, silicene, and transition metal dichalcogenide monolayers. Inspired by this interesting molecular structure, we wondered if a 2D Mo_2Pc can be constructed and if so what properties would such a 2D sheet have? Using first-principles calculations, we show that a 2D Mo_2Pc-based organometallic sheet can have unique mechanical, electronic, magnetic, and optical properties not seen in conventional organometallic monolayers containing isolated metal atoms.

II. THEORETICAL PROCEDURES

Our calculations are performed using the projector augmented wave (PAW)[9] method as implemented in Vienna Ab initio Simulation Package (VASP) code.[10] The exchange and correlation potential is treated within the generalized gradient approximation (GGA) using both the Perdew–Burke–Ernzerhof (PBE)[11] and hybrid Heyd–Scuseria–Ernzerhof (HSE06)[12,13] functional. The Monkhorst-Pack 5 × 5 × 1 special k-point meshes[14] are used for a primitive unit cell and the cutoff energy is set to be 400 eV. The criteria for convergence in energy and force are 1×10^{-4} eV and 0.01 eV/Å, respectively. A vacuum space of 20 Å is used between layers. All structural parameters of the Mo_2Pc sheet have been fully optimized. The band structure and optical properties are calculated using the hybrid HSE06 functional. To study the anisotropic characteristics of elastic constants, we adopt a rectangular cell with the same computational accuracy as above. The dependence of our method on the mesh points is tested by using a 6 × 6 × 1 k-point grid, which gives the same results as those obtained with the 5 × 5 × 1 mesh. To validate our computational method, we calculated the geometry of the

Received: November 6, 2013
Revised: November 24, 2013
Published: December 16, 2013

ACS Publications © 2013 American Chemical Society

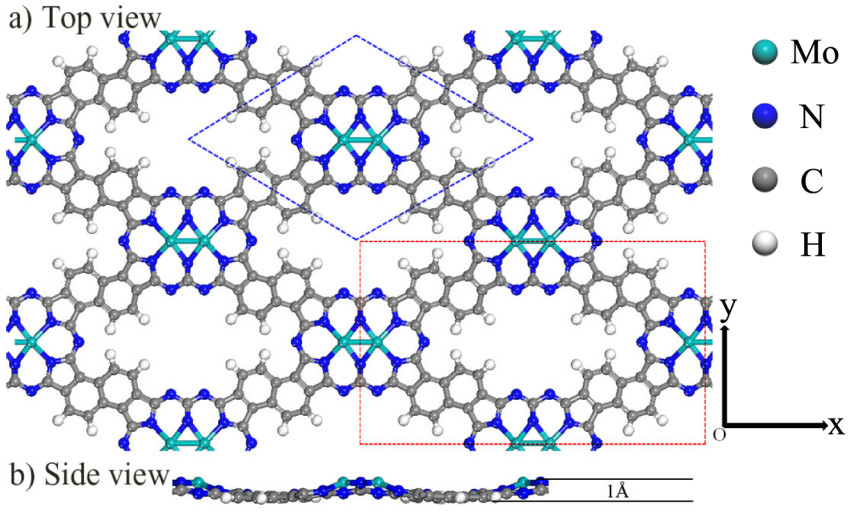

Figure 1. Geometric structures of 2D Mo_2Pc sheet. In the top view (a) the primitive unit cell is marked by blue dotted line, whereas the rectangular unit cell is marked by red dotted line. In the side view (b) the buckling is about 1 Å.

Mo_2O_2Pc. The Mo−Mo bond length is found to be 2.67 , which is in agreement with the experimental value[8] of 2.64 Å.

III. RESULTS AND DISCUSSION

A. Geometric Structures of the 2D Mo_2Pc Sheet. The calculated structure of Mo_2Pc sheet is shown in Figure 1. The optimized rhombohedral lattice parameter is 14.21 Å with an angle of 60.7° between two adjacent sides. The rectangular lattice parameters are 24.47 × 14.31 Å and the structure has *p2mm* symmetry. From the side view in Figure 1b, it can be seen clearly that the single-layer sheet is not strictly planar. Four central atoms (two Mo and two N) slightly protrude out of the plane, causing a buckling of about 1 Å. Our calculations indicate that the central Mo atoms are linked by a single bond similar to that in the molecular structure as characterized using X-ray crystal analysis.[8] The interatomic distance between the two Mo ions in the 2D structure is calculated to be 2.37 Å, which is larger than the bond length of a free Mo_2 molecule (1.70 Å), but slightly smaller than that of Mo_2Pc molecule as shown in Table 1. In the Mo_2Pc sheet, the bond lengths between Mo and amino nitrogen (pyrrole nitrogen) is 1.97 (2.08) Å.

B. Mechanical Properties. Next we study the elastic properties. For comparison we first calculate the in-plane stiffness of graphene. This is found to be 350 N/m and agrees well with the experimental value of 340 N/m.[15] Different from the metal-atom-based sheet, the metal dimer imposes anisotropy in the geometry, which in turn causes anisotropies in its mechanical properties. To examine this effect on the elastic constants of the Mo_2Pc sheet, we use a rectangular lattice cell as shown in Figure 1 (red dotted line). It is known that generally an anisotropic elastic solid has 21 independent second-order elastic constants, but only in-plane components of the stiffness tensors are meaningful for two-dimensional materials. Due to the symmetry of Mo_2Pc sheet only four elastic constants need to be considered, namely, C_{11}, C_{22}, C_{12}, and C_{66}. These are calculated to be C_{11} = 116.4 N/m, C_{22} = 43.6 N/m, C_{12} = 20.7 N/m, and C_{66} = 27.2 N/m. These values indicate that elastic property of the Mo_2Pc sheet is anisotropic as expected because it is much stiffer along the *x*-direction than along the *y*-direction due to the Mo−Mo bond.

C. Magnetic and Electronic Properties. To study the magnetic state of Mo_2Pc sheet, spin-polarized calculations are carried out. We find that unlike the Mo_2 dimer, which is nonmagnetic (NM) in free space, each of the Mo atom in the Mo_2 dimer embedded in the Pc framework carries a magnetic moment of 0.88 μ_B. Table 1 shows the changing trend of magnetic moments from Mo_2 dimer to Mo_2Pc molecule to Mo_2Pc sheet. The Mo_2 dimer has a bond length of 1.70 Å. This is consistent with previous studies[16−18] that show the bond length lies in the range 1.63−1.98 Å, but it is slightly shorter than those of the experimental values (1.93 Å).[19,20] From Table 1, we can see that the Mo−Mo distance in the Mo_2Pc molecule is very close to that in the Mo_2Pc sheet, but it is significantly stretched as compared to the Mo_2 dimer in the free state. The former indicates that the Mo−Mo interaction is not significantly affected when the molecules self-assemble to form a sheet. The enlargement in the Mo−Mo bond weakens the hybridization between two Mo atoms and, hence, induces a magnetic moment on the Mo site; the magnetic moments are coupled antiferromagnetically. In Mo_2Pc sheet the AFM state is 260 meV lower in energy than the ferromagnetic (FM) state.

Table 1. Comparison of Mo−Mo Bond Lengths (L_B), Magnetic Moment (M) on the Mo Site, and Magnetic Coupling of Mo_2 in Different Bonding Environments

structure	L_B (Å)	M (μ_B/atom)	magnetic coupling
Mo_2	1.70	0	NM
Mo_2Pc	2.42	0.94	AFM
Mo_2Pc sheet	2.37	0.88	AFM

The projected densities of states of the d electrons on Mo sites are shown in Figure 2. Note that the main contribution to the magnetic moments comes from the d_{z^2} orbitals. The AFM states in Mo_2Pc molecule and in Mo_2Pc sheet are similar to the AFM state in Cr_2O_2 molecule where the two O atoms are doubly bridged on the Cr−Cr bond.[21] Although there are four N atoms bonded with each Mo atom, the two amino nitrogen atoms are much closer to Mo−Mo and share a configuration similar to that of Cr_2O_2. Because Cr and Mo are in the same group in the periodic table with $nd^5(n+1)s^1$ (n = 3, 4)

dx.doi.org/10.1021/jp4109255 | J. Phys. Chem. A 2014, 118, 304−307

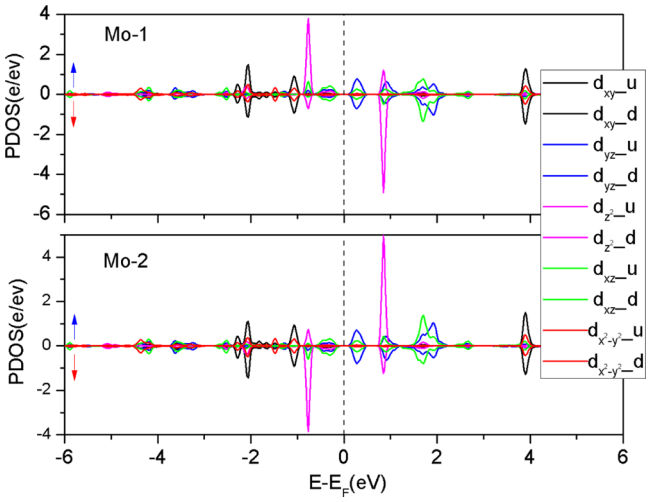

Figure 2. Projected densities of states of d orbitals for Mo-1 and Mo-2 atoms in the 2D Mo_2Pc sheet. The blue and red arrows denote spin up and spin down, respectively. The Fermi level is marked by the black dashed line.

electronic configurations, respectively, similar magnetic coupling between Cr_2O_2 and Mo_2N_2 is understandable.

The electronic structure is calculated using the hybrid HSE06 functional, which is known to yield a more accurate band gap than the PBE functional.[22] The band structure and corresponding partial density of states (PDOS) of the Mo_2Pc sheet are shown in Figure 3. We see that the valence band maximum (VBM) and conduction band minimum (CBM) are located at the K point with a direct gap of 0.93 eV. The PDOS clearly shows that p−d orbital hybridization corresponding to the Mo−N bond plays a dominant role near the Fermi level.

D. Optical Properties. To investigate the optical properties of the Mo_2Pc sheet, we have computed the optical spectra along *x* and *y* axes by calculating the frequency dependent imaginary part of the dielectric function. Again the hybrid HSE06[23] functional was used because it has been found to reproduce well the experimentally observed optical absorption spectrum of other 2D materials.[24] The calculated results are plotted in Figure 4. The peak along the *x*-direction at 1270 nm

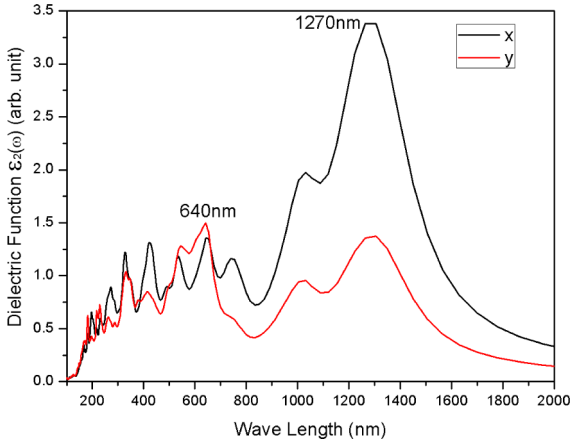

Figure 4. Wavelength dependent absorption spectra of 2D Mo_2Pc sheet along x and y axes calculated using HSE06 functional.

lies in the NIR range, whereas for the *y*-direction, the absorption peak is at 640 nm falling in the visible light range. Different from the isotropic single-atom-based transition metal−Pc molecules that absorb only visible light,[25] the Mo_2Pc sheet shows directional absorptions for visible light and NIR light, suggesting potential for applications in infrared ray detectors. On the basis of the calculated dielectric functions, we can further obtain the static refractive index $n(\omega)$ using the following equation,

$$n(\omega) = \sqrt{\frac{|\varepsilon(\omega)| + \mathrm{Re}\,\varepsilon(\omega)}{2}}$$

where $\varepsilon(\omega)$ and $\mathrm{Re}\,\varepsilon(\omega)$ denote dielectric function and its real part, respectively. The derived maximum refractive index of NIR light in the *x*- and *y*-direction is 2.14 and 1.72, respectively,

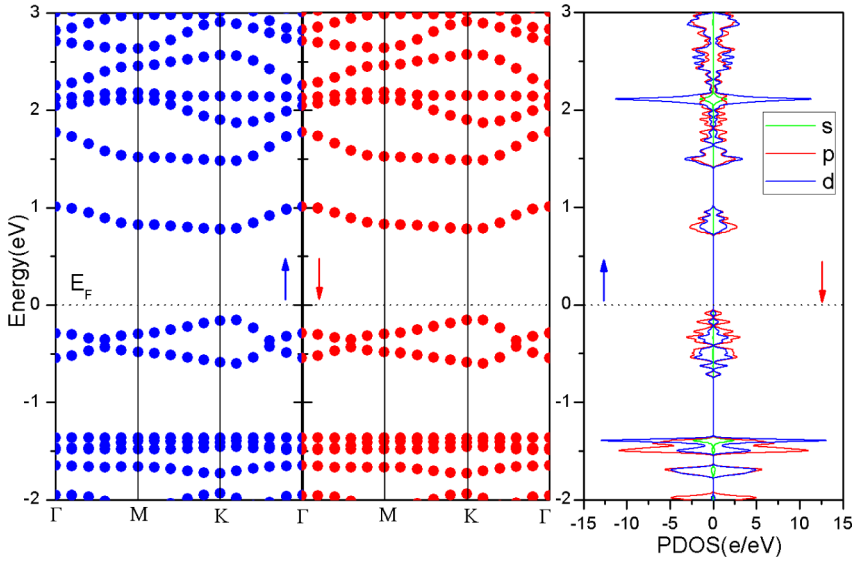

Figure 3. Spin-polarized band structures and corresponding partial density of states of the 2D Mo_2Pc sheet. Γ, M, and K are high symmetry points in the reciprocal space. The Fermi level (E_F) is set to zero and marked with the dotted line. The blue and red arrows denote spin up and down, respectively.

dx.doi.org/10.1021/jp4109255 | J. Phys. Chem. A 2014, 118, 304−307

suggesting that the NIR light would travel 1.24 times slower in the *x*-direction than in the *y*-direction.

IV. CONCLUSION

In summary, inspired by the recent experimental advances in synthesizing Mo_2–phthalocyanine molecular structures, we explored the structure and properties of a corresponding periodic 2D-like system. The following conclusions are drawn: (1) The Mo_2Pc sheet shows anisotropic elasticity with the elastic constant in the *x*-direction being about 3 times of that in the *y*-direction. (2) The Mo_2Pc sheet is a semiconductor with a direct band gap of 0.93 eV. (3) When the nonmagnetic Mo_2 dimer is embedded in the Pc substrate, the Mo–Mo bond is stretched significantly, thus inducing 0.88 μ_B magnetic moment on each Mo site with antiferromagnetic coupling. (4) The optical spectra of the Mo_2Pc sheet display anisotropic absorptions both in the visible and in the near-infrared regions. In the *x*-direction, the NIR absorption intensity is about 2.5 times that of visible light, but they have similar intensities in the *y*-direction. The corresponding refractive index of NIR light in the *x*-direction is about 1.24 times that in the *y*-direction. The displayed intrinsic anisotropies in the metal-dimer-based organometallic sheet may have promising applications in mechanical and optical devices. We hope that the present study stimulates further experimental efforts in synthesizing metal-dimer-based porous organometallic sheets.

AUTHOR INFORMATION

Corresponding Author

*Corresponding Author E-mail: sunqiang@pku.edu.cn.

Notes

The authors declare no competing financial interest.

ACKNOWLEDGMENTS

This work is partially supported by grants from the National Natural Science Foundation of China (NSFC-21173007 and 11274023), and from the National Grand Fundamental Research 973 Program of China (2012CB921404). P.J. acknowledges the support of the Department of Energy, Office of Basis Energy Sciences, Division of Materials Sciences and Engineering under Award # DE-FG02-96ER45579.

REFERENCES

(1) Colson, J. W.; Woll, A. R.; Mukherjee, A.; Levendorf, M. P.; Spitler, E. L.; Shields, V. B.; Spencer, M. G.; Park, J.; Dichtel, W. R. Oriented 2D Covalent Organic Framework Thin Films on Single-Layer Graphene. *Science* **2011**, *332*, 228–231.

(2) Spitler, E. L.; Dichtel, W. R. Lewis acid-catalysed formation of two-dimensional phthalocyanine covalent organic frameworks. *Nat. Chem.* **2010**, *2*, 672–677.

(3) Chui, S. S.-Y.; Lo, S. M.-F.; Charmant, J. P. H.; Orpen, A. G.; Williams, I. D. A Chemically Functionalizable Nanoporous Material $[Cu_3(TMA)_2(H_2O)_3]_n$. *Science* **1999**, *283*, 1148–1150.

(4) Grill, L.; Dyer, M.; Lafferentz, L.; Persson, M.; Peters, M. V.; Hecht, S. Nano-architectures by covalent assembly of molecular building blocks. *Nat. Nano.* **2007**, *2*, 687–691.

(5) Kambe, T.; Sakamoto, R.; Hoshiko, K.; Takada, K.; Miyachi, M.; Ryu, J.-H.; Sasaki, S.; Kim, J.; Nakazato, K.; Takata, M.; Nishihara, H. π-Conjugated Nickel Bis(dithiolene) Complex Nanosheet. *J. Am. Chem. Soc.* **2013**, *135*, 2462–2465.

(6) Wang, Z. F.; Liu, Z.; Liu, F. Organic topological insulators in organometallic lattices. *Nat. Commun.* **2013**, *4*, 1471.

(7) Abel, M.; Clair, S.; Ourdjini, O.; Mossoyan, M.; Porte, L. Single Layer of Polymeric Fe-Phthalocyanine: An Organometallic Sheet on Metal and Thin Insulating Film. *J. Am. Chem. Soc.* **2010**, *133*, 1203–1205.

(8) Matsushita, O.; Derkacheva, V. M.; Muranaka, A.; Shimizu, S.; Uchiyama, M.; Luk'yanets, E. A.; Kobayashi, N. Rectangular-Shaped Expanded Phthalocyanines with Two Central Metal Atoms. *J. Am. Chem. Soc.* **2012**, *134*, 3411–3418.

(9) Blöchl, P. E. Projector augmented-wave method. *Phys. Rev. B* **1994**, *50*, 17953–17979.

(10) Kresse, G.; Furthmüller, J. Efficient iterative schemes for ab initio total-energy calculations using a plane-wave basis set. *Phys. Rev. B* **1996**, *54*, 11169–11186.

(11) Perdew, J. P.; Burke, K.; Ernzerhof, M. Generalized Gradient Approximation Made Simple. *Phys. Rev. Lett.* **1996**, *77*, 3865–3868.

(12) Heyd, J.; Scuseria, G. E.; Ernzerhof, M. Hybrid functionals based on a screened Coulomb potential. *J. Chem. Phys.* **2003**, *118*, 8207–8215.

(13) Heyd, J.; Scuseria, G. E.; Ernzerhof, M. Erratum: "Hybrid functionals based on a screened Coulomb potential" [J. Chem. Phys. [118], 8207 (2003)]. *J. Chem. Phys.* **2006**, *124*, 219906–1.

(14) Monkhorst, H. J.; Pack, J. D. Special points for Brillouin-zone integrations. *Phys. Rev. B* **1976**, *13*, 5188–5192.

(15) Lee, C.; Wei, X.; Kysar, J. W.; Hone, J. Measurement of the Elastic Properties and Intrinsic Strength of Monolayer Graphene. *Science* **2008**, *321*, 385–388.

(16) Andzelm, J.; Radzio, E.; Salahub, D. R. Model potential calculations for second-row transition metal molecules within the local-spin-density method. *J. Chem. Phys.* **1985**, *83*, 4573–4580.

(17) Boudreaux, E. A.; Baxter, E. SCMEH-MO calculations on Cr_2 and Mo_2 molecules. *Int. J. Quantum Chem.* **2001**, *85*, 509–513.

(18) Zhang, W.; Ran, X.; Zhao, H.; Wang, L. The nonmetallicity of molybdenum clusters. *J. Chem. Phys.* **2004**, *121*, 7717–7724.

(19) Efremov, Y. M.; Samoilova, A. N.; Kozhukhovsky, V. B.; Gurvich, L. V. On the electronic spectrum of the Mo_2 molecule observed after flash photolysis of $Mo(CO)_6$. *J. Mol. Spectrosc.* **1978**, *73*, 430–440.

(20) Hopkins, J. B.; Langridge-Smith, P. R. R.; Morse, M. D.; Smalley, R. E. Supersonic metal cluster beams of refractory metals: Spectral investigations of ultracold Mo_2. *J. Chem. Phys.* **1983**, *78*, 1627–1637.

(21) Reddy, B. V.; Khanna, S. N. Chemically Induced Oscillatory Exchange Coupling in Chromium Oxide Clusters. *Phys. Rev. Lett.* **1999**, *83*, 3170–3173.

(22) Deák, P.; Aradi, B.; Frauenheim, T.; Janzén, E.; Gali, A. Accurate defect levels obtained from the HSE06 range-separated hybrid functional. *Phys. Rev. B* **2010**, *81*, 153203.

(23) Gajdoš, M.; Hummer, K.; Kresse, G.; Furthmüller, J.; Bechstedt, F. Linear optical properties in the projector-augmented wave methodology. *Phys. Rev. B* **2006**, *73*, 045112.

(24) Du, A.; Sanvito, S.; Li, Z.; Wang, D.; Jiao, Y.; Liao, T.; Sun, Q.; Ng, Y. H.; Zhu, Z.; Amal, R.; Smith, S. C. Hybrid Graphene and Graphitic Carbon Nitride Nanocomposite: Gap Opening, Electron–Hole Puddle, Interfacial Charge Transfer, and Enhanced Visible Light Response. *J. Am. Chem. Soc.* **2012**, *134*, 4393–4397.

(25) de la Torre, G.; Vázquez, P.; Agulló-López, F.; Torres, T. Role of Structural Factors in the Nonlinear Optical Properties of Phthalocyanines and Related Compounds. *Chem. Rev.* **2004**, *104*, 3723–3750.